

Gas Sensor of Au/AgNPs/PSi/c-Si Using Pulsed Laser Ablation Using a YAG: Nd Laser

Wisam J. Aziz¹, Sabah J. Mezher², Saad N. Ibrahim³

^{1,2,3}Physics Department, College of Science, Al-Mustansiriyah University, Baghdad, Iraq

Abstract: Pulsed laser ablation in liquid was employed to synthesize silver nanoparticle (Ag). Silver nanoparticles are synthesized by pulsed laser ablation of high purity zinc target in double distilled water with 36.924 J/cm^2 laser fluencies at RT. UV-visible absorption and transmission electron microscope are used for the characterization of silver nanoparticle (NPs). The optical properties, size, and the morphology of the synthesized silver nanoparticle were influenced strongly by laser fluence and wavelength. The use of water gave spherical silver nanoparticle NPs with average size 16 nm. The absorbance spectrum of the silver nanoparticles solution displays a quasisymmetric absorption band centered at 417 nm, which indicates that the nanoparticles in the growth solution are quasispherical approximately 8 nm in size. The silver nanoparticles, was faint yellow in color. It is expected, that the obtained results will find applications in the synthesis of new materials with modified properties, in the fabrication of catalysts with optimized selectivity and efficiency, in medicine for preparation of nanoparticle-based probes with great potential for targeting, imaging and treating different diseases etc. Chemical interaction between the (100-400 ppm) vapor methanol gas and Au/Ag NPs/p-PSi/c-Si device surface caused to some of variations in the output signal recorded as resistance decrease of device at room temperature.

Keyword: Ag nanoparticle, SEM, Gas sensor, PSi.

1. Introduction

Last year's considerable efforts have been directed to preparation and investigation of nanostructured materials. Broadly defined, nanostructured materials are solids composed of structural elements (mostly crystallites) which characteristic size falls in the range of 1 – 100 nm [1]. Noble metal nanoparticles NPs such as Ag have been a source of great interest due to their novel electrical, optical, physical, chemical and magnetic properties [2, 3]. They were very attractive for biophysical, biochemical, and biotechnological applications due to their unusual physical properties, especially due to their sharp Plasmon absorption peak at the visible region. Another important advantage Ag nanoparticles prepared by PLAL process were stable for a period of months. Additionally, silver nanoparticles are chemically stable and typically exhibit surface enhanced Raman scattering SERS in the visible wavelength range, where they may cause a tremendous increase in various optical cross-sections. The resonance frequencies strongly depend on particle shape and size as well as on the optical properties of the material within the near-field of the particle [4]. As well as, Silver has been for thousands of years was used as a disinfectant; from the other side nobody can neglect its value as a catalyst [5]. When a laser pulse reaches a sample surface, some of the energy is reflected by the surface. It is noted that the reflectivity depends on the material and laser wavelength [6]. The energy absorbed by the sample is transferred from optical photons to electrons and then to the lattice, which then diffuses the energy into the material [7]. Extremely high energy pulses may cause photochemical reactions which remove atoms and molecules from the surface. The heated surface can reach temperatures close to the critical temperature and cause rapid vaporization process. The vaporization resulting in plasma that consists of ionized vaporized atoms and electrons. It is possible that the plasma cloud absorbs some of the incident laser energy and thereby only allows a fraction of the laser energy to reach the surface (plasma

shielding). The plasma expands and is heated by photon absorption. Later the vapour cools and aerosol particles begin to form. The rest of the energy diffuses into the material via heat transfer. Depending on the applied laser energy, the surface may be melted into a liquid with a moving solid-liquid interface. Liquid may be removed from the molten pool as droplets that result in a higher ablation rate. The absorption of laser light by metal nanoparticles gives rise to a succession of energy transformation processes. These involve the successive excitation and relaxation of the metal electrons, its interaction with the lattice, i.e. electron-phonon relaxation and the phonon-phonon thermalization. Afterwards, several thermal processes like melting or evaporation can be activated. The heat diffusion from the metal particle to the support takes place on a time scale much shorter than the pulse width. This enables a simple thermodynamic treatment of the laser induced temperature rise [8, 9].

2. Experimental Section

For electrochemical anodization, boron doped p-type silicon substrate of <100> orientation with resistivity (0.01-0.02) $\Omega \cdot \text{cm}$ was used. For anodization, constant DC current source is used with electrolyte solution containing 1:1:2 ratio of HF (48%): DI water: Ethanol respectively. The electrochemical cell used has two electrode configurations with a platinum electrode as cathode and silicon wafer as anode. As the starting material was of p-type silicon substrate hence, anodization was carried out at room temperature in the dark. p-type porous silicon samples were fabricated at anodization time 4 min and current density 40 mA/cm^2 . In contrast, the cell is called ECE if the p-type c-Si samples were not illuminated. The samples were rinsed first with pentane, then with 98 % methanol and finally with deionized water (18.5 M Ω -cm). Next, the samples were dried at about 60°C on a hot plate rather than drying in the N₂ nozzle in order to avoid cracking and peeling of the PSi layer.

Fig. 1 shows the experimental setup for laser ablation of solid metal target immersed in distilled water (DW), Nd-YAG laser 1064nm wavelength was used. Q-switched Nd-YAG laser system type HUAFEI providing pulses of 1064nm wavelength with maximum energy per pulse of 1000 mJ, pulse width of 10 ns, repetition rate of 10 Hz and effective beam diameter of 5 mm, was used for laser ablation. The laser is applied with a lens with 110 mm focal length used to achieve high laser fluence. Silver NPs were synthesized by pulsed laser ablation on a piece of silver metal plate (ounces: 99.999%) placed on the bottom of holder, vessel containing 1ml of DW. The spot size of the laser beam on the surface of the metal plate of 0.5 mm in radius(r). The laser fluence (F) was 36.924 J/cm^2 where:

$$F = \frac{\text{Pulse energy}}{A} \text{ \& } A = 2\pi r^2 \quad (1)$$

The pulse energy was 580 mJ/cm^2 . The pulse duration and the repetition rate of the laser pulse were 10 ns and 10 Hz respectively. The number of laser shots applied for the metal target was 35 pulses. The silicon p-type substrate used after it has been cleaned by a chemical etching Process. The deposition Process for one drop of Ag nanoparticles was hold on porous silicon substrate by using thermal deposition process for the purpose drying samples then hold the samples measurements. Absorbance spectra (SPE spectra) of NPs solution were measured by UVVIS double beam spectrophotometers, CECIL C. 7200 (France) and SHIMADZU. All spectra were measured at room-temperature in a quartz cell with 1 cm optical path. Additionally, spectrophotometer was used to estimate of metals nanoparticles [13]. Then The thermal evaporation system (Edwards) has been used to evaporate the high purity (99.9 %) gold on silver NPs/p-PSi/c-Si device under low pressure (about 10^{-6} torr).

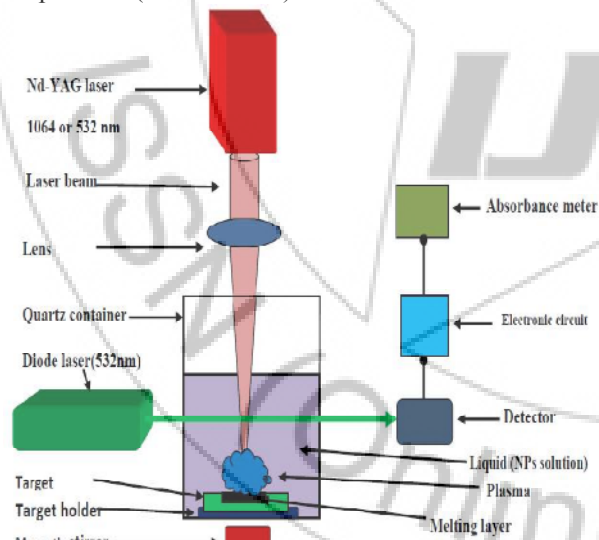


Figure 1: The experimental setup for laser ablation of Ag metal

3. Results and Discussion

The structure and lattice parameters of Ag NWs are analyzed by a LabX XRD 6000 SHIMADZU XR – Diffractometer with Cu $K\alpha$ radiation (wavelength 1.54059 \AA , voltage 30 kV, current 15 mA, scanning speed = $4^\circ/\text{min}$). The crystallinity of the produced material was characterized using X-ray diffraction (XRD). Four peaks

could be recognized in Fig. 2, the film is polycrystalline according to the ASTM standards where (111) Ag could be recognized. The peak can be indexed to the face-centered cubic (fcc) phase of silver (JCPDS file No. 04-0783). No impurities can be identified from this pattern. The calculated lattice constant according to the (1 1 1) peak is 4.08 \AA which is closely consistent with the standard value (4.086 \AA).

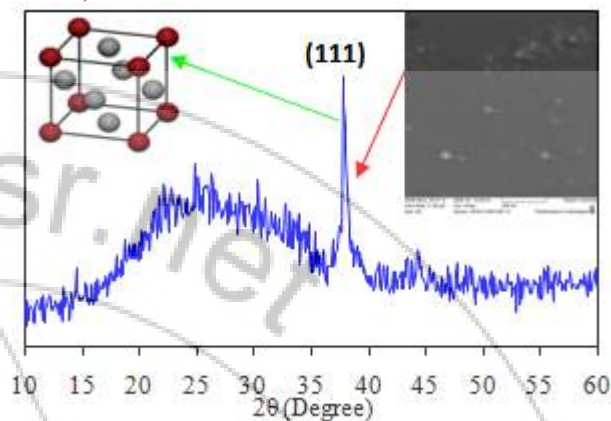


Figure 2: XRD pattern of silver nanoparticles produced by 1064-nm laser ablation ($E=1000 \text{ mJ/pulse}$) of silver plate immersed in 1ml of DDDW. The laser shots set of 35 pulses, respectively.

The effect of laser irradiation on colloidal solution examined by measuring absorption spectra which is shown in Fig. 3. The spectra exhibited absorption bands with a maximum around 417 nm , which is typical for the excitation at the Plasmon resonance in silver nanoparticles and weak absorption due to inter-band transitions in the region less than 300 nm . A comparison of absorbance of inter-band transitions at this region indicates that the formation efficiencies of colloids increase with an increase in the laser wavelength under our conditions. The bandwidth of the plasmon resonance is significantly reduced and the narrowing of the plasmon bandwidth is accompanied by an increase in the absorption magnitude. An observed narrowing of the Ag plasmon resonance band can be attributed to the redistribution of the particle sizes narrowing of the particle size dispersion, its increase in intensity can be assigned to the increase of the particle concentration in the solution. A recorded growth of absorption in the 417 nm region can be attributed to the increase of a particle concentration in result of a fragmentation of larger clusters that selectively absorb the incident laser radiation. When the particles were subjected to 417 nm laser excitation, the position of the plasmon peak shifted to the blue region and the bandwidth was reduced. These changes of the absorption spectrum suggest that the mean particle dimension and the size distribution are reduced by laser irradiation [14-16]. The presence of the single surface-plasmon peak implies that the silver nanoparticles are spherical [17]. Typically the laser exposure of a metal target immersed into a liquid leads to the dispersion of the metal nanoparticles into the surrounding liquid, if the laser fluence is sufficiently high. The rate of NP generation depends not only on the laser fluence but also of experimental parameters such as the metal reflectivity at the laser wavelength, the nature of the liquid, etc. The rate of NP production decreases with the laser fluence. At lower fluence the rate of NP generation drops,

while the surface of the target undergoes eye-visible changes. The coloration of the exposed areas is well pronounced while the target remains in the liquid, whereas it fades if the target is removed from the liquid and dried. In case of the Ag target the color of laser-treated areas is yellow.

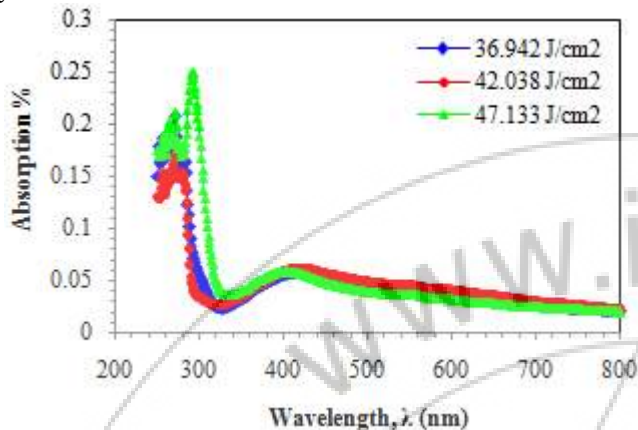


Figure 3: Absorption as function of wavelength of silver nanoparticles produced by 1064-nm laser ablation ($E=1000$ mJ/pulse) of silver plate immersed in 1ml of DDDW.

Fig. 4 shows the SEM images and the corresponding size distributions of silver nanoparticles produced by laser ablation of a silver plate immersed in 1 ml of DDDW, at 35 pulses, respectively. The Nd-YAG laser of 1064 nm and energy of 1000 mJ was used. The nanoparticles thus produced were calculated to have an average diameter of 16 nm at 35 pulses, respectively. The result revealed that the average diameter of nanoparticles increase with an increase in laser shots.



Figure 4: SEM images and size distribution of silver nanoparticles produced by 1064-nm laser ablation ($E=1000$ mJ/pulse) of silver plate immersed in 1ml of DDDW. The laser shots set of 35 pulses, respectively.

The vapor methanol gas sensor sensitivity of Au/Ag NPs/p-PSi/c-Si as shown in Fig.5. Chemical interaction between the (100-400 ppm) vapor methanol gas and Au/Ag NPs/p-PSi/c-Si device surface caused to some of variations in the output signal recorded as resistance decrease of device at room temperature.

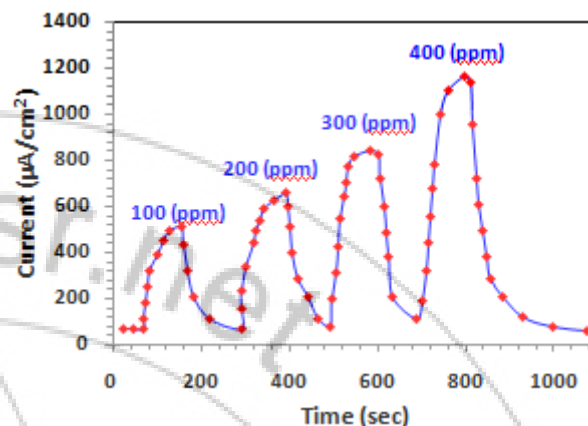


Figure 5: Relation between current and time of Au/Ag NPs/p-PSi/c-Si with different vapor methanol gas concentration.

4. Conclusions

1. The absorbance spectrum of the silver nanoparticles solution displays a quasisymmetric absorption band centered at 417 nm, which indicates that the nanoparticles in the growth solution are quasispherical approximately 8 nm in size. The silver nanoparticles, was faint yellow in color.
2. It is expected, that the obtained results will find applications in the synthesis of new materials with modified properties, in the fabrication of catalysts with optimized selectivity and efficiency, in medicine for preparation of nanoparticle-based probes with great potential for targeting, imaging and treating different diseases etc.
3. The sensitivity of Au/Ag NPs/p-PSi/c-Si to (100-400) ppm vapor methanol gas as a function of working time. As evident, the sensitivity increases with the vapor methanol gas concentration.

References

- [1] Kreibig, U.; Vollmer, M. Optical Properties of Metal Clusters; Springer Series in Material Science 25; Springer: Berlin, (1995).
- [2] T. Tsuji et al. / Journal of Photochemistry and Photobiology A: Chemistry 145 (2001) 201–207
- [3] T. Tsuji et al. / Applied Surface Science 202 (2002) 80–85
- [4] P. Sen, J. Ghosh, A. Abdullah, P. Kumar, Vandana (Preparation of Cu, Ag, Fe and Al nanoparticles by the exploding wire technique) Proc. Indian Acad. Sci. (Chem. Sci.)115, (2003) 499–508.
- [5] J. Priklulis, F. Svedberg, M. Kall (Optical Spectroscopy of Single Trapped Metal Nanoparticles in Solution) Nano Letters 4 (2004) 115-118.

- [6] C. Liu (A study of particle generation during laser ablation with applications) Doctoral Thesis, University of California, Berkeley, (2005), (1-189).
- [7] N.V. Tarasenko et al. / Applied Surface Science 247 (2005) 418–422
- [8] A. R. Siekkinen, J. M. McLellan, J. Chen, Y. Xia (Rapid synthesis of small silvernanocubes by mediating polyol reduction with a trace amount of sodium sulfide or sodium hydrosulfide) Chemical Physics Letters 432 (2006) 491–496.
- [9] X. Zheng, W. Xu, C. Corredor, S. Xu, J. An (Laser-Induced Growth of Monodisperse Silver Nanoparticles with Tunable Surface Plasmon Resonance Properties and a Wavelength Self-Limiting Effect) J. Phys. Chem. 111 (2007) 14962-1496
- [10] D. B. Sanchez (The Surface Plasmon Resonance of Supported Noble Metal Nanoparticles: Characterization, Laser Tailoring, and SERS Application), PhD thesis, Madrid University (2007).
- [11] W. Chan, R. S. Averback, D. G. Cahill and A. Lagoutchev (Dynamics of femtosecond laser-induced melting of silver) physical review B 78 (2008) 214107.
- [12] M. S. Charget, A. Gruszecka, A. Smolira, J. Cytawa, L. Michalak (Mass spectrometric investigations of the synthesis of silver nanoparticles via electrolysis) Vacuum 82 (2008) 1088–1093.
- [13] L. V. Zhigilei, Z. Lin and D. S. Ivanov (Atomistic Modeling of Short Pulse Laser Ablation of Metals: Connections between Melting, Spallation, and Phase Explosion) J. Phys. Chem. C 113 (2009) 11892–11906.
- [14] K. Zimmer (Analytical solution of the laser-induced temperature distribution across internal material interfaces) International Journal of Heat and Mass Transfer 52 (2009) 497–503
- [15] T. Ctvrtnickova, L. Cabalin, J. Laserna, V. Kanicky, G. Nicolas (Laser ablation of powdered samples and analysis by means of laser-induced breakdown spectroscopy) Applied Surface Science 255 (2009) 5329–5333.
- [16] K. Gouriet, M. Sentis and T. E. Itina (Molecular Dynamics Study of Nanoparticle Evaporation and Condensation in a Gas) J. Phys. Chem. C 113 (2009) 18462–18467.
- [17] V. Amendola and M. Meneghetti (Size Evaluation of Gold Nanoparticles by UVVIS Spectroscopy) J. Phys. Chem. C 113 (2009) 4277–4285.